P2A.4 On the vertical profile of stratus liquid water flux using a millimeter cloud radar

Shelby Frisch[1]*, and Paquita Zuidema[2]
[1] NOAA/Environmental Technology Laboratory and Colorado State University
[2] NOAA/Environmental Technology Laboratory and University of Colorado

1. Introduction

There are two components of the vertical flux of liquid water in stratus clouds, one component is due to the mean fall velocity of the cloud droplets, also referred to as gravitational settling, while the other is due to any turbulent motion which can redistribute the cloud droplets. Previous work has shown these two terms can be comparable in magnitude, even for non-drizzling cloudy portions (Nicholls, 1984). Nicholls (1984) also found that calculations of the implied cloud-top entrainment flux were sensitive to the liquid water flux term, because the liquid water flux offsets the apparent upward moisture flux. A correct treatment of the total water flux and entrainment flux, both in modeling and data analysis, must therefore also include the droplet settling term.

Since millimeter cloud radars can detect these droplets, cloud microphysical retrievals can be used to estimate the stratus cloud droplet liquid water flux. Earlier retrievals using cloud radars have been used to retrieve the effective radius from the reflectivity measurements. By using additional information about cloud droplet fall velocities in the Stokes range, we can estimate the liquid water flux in the non-drizzling portion of stratus clouds.

Furthermore, by taking the divergence of the gravitational settling term, we can calculate the associated latent heating and cooling rates. These can be compared to the radiative heating rates calculated from similarly-retrieved liquid water contents and effective radii, as one measure of the relative impact of gravitational settling upon the total diabatic heating. The knowledge of both diabatic heating terms also provides useful constraints on the modeling of mixed-layer clouds.

In this initial investigation we focus upon a non-drizzling stratus day observed during the stratocumulus leg of the East Pacific Investigation of Climate (EPIC), held during October 2001 in the southeastern Pacific region. This two-week ship-based stratocumulus study, discussed further in Bretherton et al. (2003), included in its goals an increased understanding of the heat and water fluxes for this region, and the measurement of the vertical structure of the atmospheric boundary layer.

2. Method

The vertical motion of the cloud droplets w can be written as the combination of the droplet fall velocity plus the vertical turbulent air motion, or $w_t + w'$ respectively. The total mean vertical liquid water flux is

$$\overline{q_l w} = \overline{q_l w_t} + \overline{q_l' w'} \tag{1}$$

The first term on the right hand side is liquid water flux due to the fall velocity of the cloud droplets, and the second term is the vertical turbulent liquid water flux. The overbar represents a time or space average. We will show that the liquid water flux due to the cloud fall velocity can be evaluated using cloud radar reflectivity measurements and what is known about stratus cloud properties. This flux can be written as

$$\overline{q_l w_t} = \frac{4\pi}{3} N \rho_l \int_0^\infty r^3 w_t(r) f(r) dr \tag{2}$$

where r is the droplet radius, $f(r)$ is the droplet distribution, N is the droplet concentration, and ρ_l is the density of liquid. For non-drizzling cloud droplets, we can assume that the fall velocity will be in the Stokes range, that is $w_t \leq$0.4 ms^{-1}. Beard and Pruppacher (1969) show that the terminal velocity of a sphere for Stokes flow is

$$w_t(r) = \frac{2}{9}[g(\rho_l - \rho_a)\eta] r^2 \tag{3}$$

where g is the acceleration due to gravity, η is the viscosity of air, and ρ_a is the density of air. Substituting (3) into (2) and noting that $\rho_l \gg \rho_a$ we have

$$\overline{q_l w_t} = \frac{8\pi}{27\eta} N \rho_l^2 g < r^5 > \tag{4}$$

where $< r^5 >$ is the fifth moment of r.

For a log-normal droplet distribution, the moments of r become

$$< r^k > = r_o^k exp(k^2 \sigma_x^2 / 2) \tag{5}$$

(Frisch et al., 1995), where r_o is the logarithmic mean droplet radius and σ_x is the logarithmic spread of the droplet distribution.

Using (5), the vertical liquid water flux (4) is

$$\overline{q_l w_t} = \frac{8\pi}{27\eta} N \rho_l^2 g r_o^5 exp(25\sigma_x^2/2) \tag{6}$$

Frisch et al. (2002) show that the effective radius of log-normally distributed stratus cloud droplets can be related to the radar reflectivity through

$$r_e = \frac{1}{2}(\frac{Z}{N})^{\frac{1}{6}} exp(-0.5\sigma_x^2) \tag{7}$$

where r_e is defined as

$$r_e = \frac{< r^3 >}{< r^2 >} \tag{8}$$

* *Corresponding author address:* Shelby Frisch, R/ET6, 325 Broadway, Boulder, CO 80305 email: shelby.frisch@noaa.gov

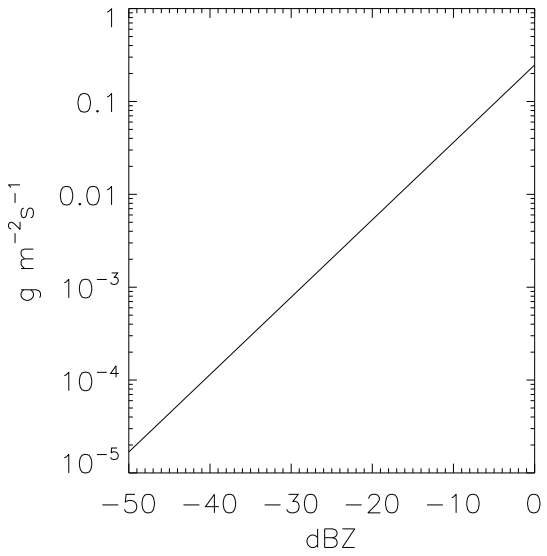

FIG. 1: Liquid water flux as a function of radar reflectivity (in dBZ) using eqn. 10. Note $dBZ = 10log_{10}(Z)$

and is related to the median radius by

$$r_o = r_e exp(-\frac{5}{2}\sigma_x^2) \tag{9}$$

Substituting (7) and (9) into (6) gives

$$\overline{q_l w_t} = \frac{\pi}{128\eta} N^{\frac{1}{6}} \rho_l^2 g Z^{\frac{5}{6}} exp(-2.5\sigma_x^2) \tag{10}$$

Frisch et al. (1995) noted that σ_x was about 0.35, which was further confirmed by Frisch et al. (2002) to be 0.32 ±0.09. They also found a range of N for marine clouds from 10 to 400 cm^{-3}, with a mean of 98 cm^{-3} and a standard deviation of 78 cm^{-3}. Since the dependence on N is to the 1/6 power, large variations in N will produce much smaller variations in the flux. Using these mean and standard deviations, we estimate the error in the flux to be about 38% for marine stratus clouds. The biggest contribution is from the variation in σ_x . Note that the gravitational settling term is close to a linear function of the radar reflectivity.

In order to use Eqn. 10, we must be careful to stay within the Stokes range where the radius is less than 40 microns. Frisch et al. (1995) used a threshold of -17 dBZ to separate drizzle from non-drizzle, and did not do any retrievals when the radar reflectivity was above this value. Less than one percent of the droplets will have a size greater than 30 microns, for a lognormal distribution and the above values for N and σ_x for marine stratus. Figure 1 shows a plot of the liquid water flux vs radar reflectivity from equation (10) for marine stratus clouds using σ_x =0.35 and N=100. At about -17 dBZ, the maximum liquid water flux is 0.02 g m^{-2} s^{-1}.

For horizontally homogeneous clouds, the time rate of change of the liquid water is the vertical gradient of the liquid water flux. The associated latent heating can then be estimated as

$$\frac{\partial T}{\partial t} = -\frac{L}{\rho_a c_p} \frac{\partial \overline{q_l w_t}}{\partial z} \tag{11}$$

where T is temperature, L is the latent heat of vaporization, and c_p is the heat capacity of air at constant pressure. Complete evaporation of a liquid water flux of 0.02 g m^{-2} s^{-1} within a radar range gate of 45 m generates a latent cooling rate of about 3.0 K/hr. In practice, a centered finite difference calculation of the vertical gradient in $\overline{q_l w_t}$ is performed; the differencing accounts for an estimated latent heating error of 54%.

3. Results

An example is made of October 10, 2001. This was near the beginning of the stratocumulus study, and the research vessel was due west of the Galapagos Island at the equator and 95° W. No drizzle was observed at the surface that day, and a cloud droplet concentration of 80 cm^{-3} was inferred from combining the microwave-derived liquid water path with solar transmission measurements (see Fig. 7, Bretherton et al. (2003)). This value for N was low compared to other days, and may correspond to larger drops and higher liquid water fluxes for this day than if higher droplet concentrations were present. Throughout the cruise, more drizzle was observed during days with low droplet concentrations (Bretherton et al., 2003).

Figure 2a shows the cloud radar reflectivities measured that day and includes a surface-based ceilometer-derived cloud base. The ceilometer cloud base estimate relies on a vertical gradient in the backscattered intensity. Stratus clouds are characterized by ill-defined cloud bases of low liquid water content, leading the ceilometer algorithm to place the cloud base higher than the cloud radar.

Fig. 2b shows the liquid water flux corresponding to the gravitational settling of non-drizzling cloud drops, calculated using Eqn. 10 for N=80 cm^{-3} and an assumed σ_x of 0.35. Although no surface drizzle was observed, some radar reflectivities exceeded the drizzle threshold of -17 dBZ; liquid water flux values were not calculated for these range gates. The ceilometer cloud base heights are also shown. The liquid water flux is a maximum above the cloud base in the lower half of the cloud. Even for this mostly non-drizzling cloud a liquid water flux below the cloud base is evident.

Figure 3 shows the latent heating field estimated from Eqn. 11, with the vertical gradient in the liquid water flux calculated from the liquid water flux difference between the radar range gates lying above and below the target radar range gate, and divided by the radar vertical resolution of 45 m. The latent heating ranges from about -6 to +6 K/day. Condensational heating is evident in-cloud until near the cloud base, with evaporative cooling occurring at and below the cloud base. The latent heating is a

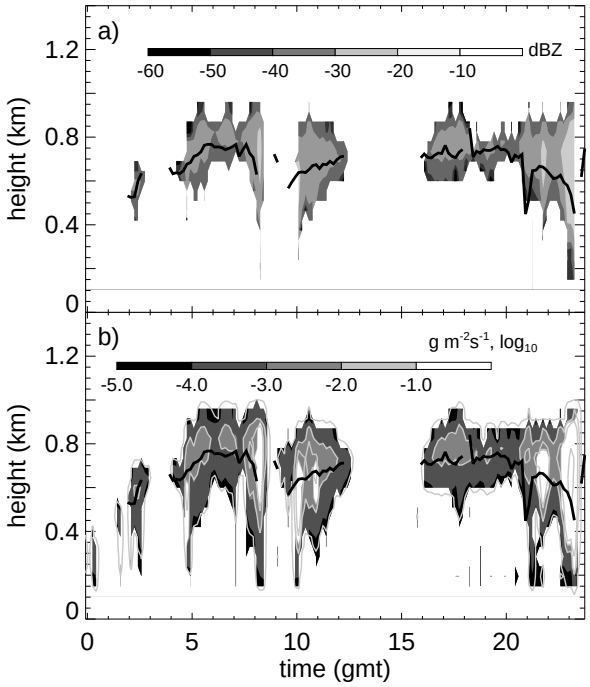

FIG. 2: a) The October 10, 2001 radar reflectivity field, and b) the corresponding liquid water flux. The ceilometer-derived cloud base heights are shown as a black line, and approximate liquid water contours, calculated for N=80 and σ_x=0.35, are shown for values of 0.01, 0.1, and 0.2 g m^{-3}. No liquid water flux values are shown for radar reflectivities exceeding the drizzle threshold of -17 dBZ.

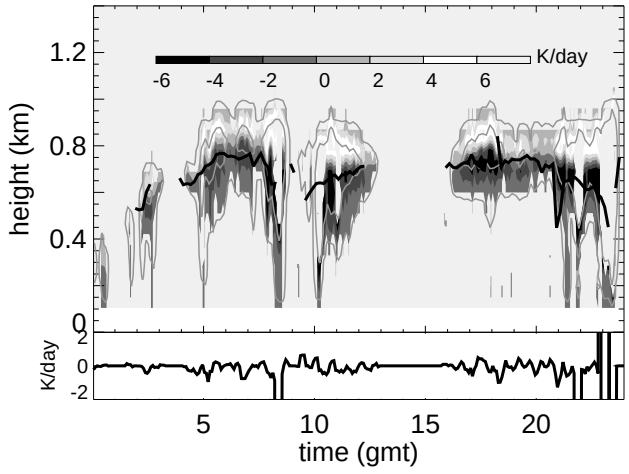

FIG. 3: Top panel: similar to Fig. 2b but showing the corresponding latent heating in K/day, with approximate liquid water contents contours at 0.01 and 0.1 g m^{-3}. Bottom panel shows the vertically-integrated latent heating, in K/day.

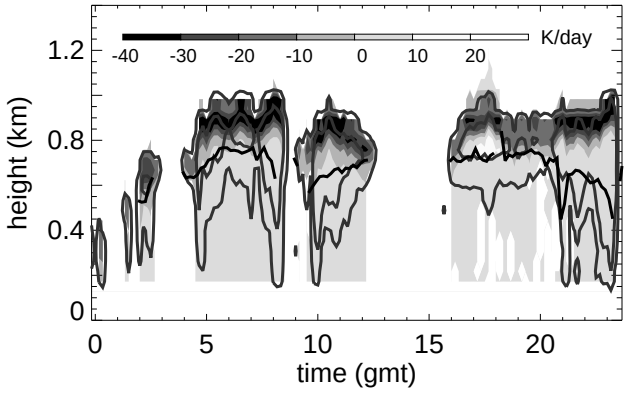

FIG. 4: Similar to Fig. 3, but showing the net radiative heating field, calculated as longwave+shortwave - longwave$_{clearsky}$ - shortwave$_{clearsky}$.

maximum somewhat below cloud top, and the latent cooling a maximum around the cloud base. As shown in the lower panel, the vertically-integrated latent heating rate is often near zero. This is consistent with the total water content (the sum of the water vapor and liquid water) remaining constant with height.

The net broadband radiative heating rates were calculated, to help assess the relative importance of the latent heating. This is shown in Figure 4 as the sum of the longwave and shortwave heating, minus the clear-sky shortwave and longwave heating. The radiative heating rates were calculated using the model Streamer (Key, 2001). Values for the liquid water content and effective radii were retrieved using the Frisch et al. (1995) method and the same values for N and σ_x as used for the latent heating calculation. The temperature and relative humidity structure were interpolated and extrapolated from the available soundings (15 and 18 GMT). Solar noon occurred at about 17:40 GMT, and is evident in Fig. 4 as a time period with lessened cloud-top cooling and enhanced within-cloud warming. The radiative heating rates in vertical columns previously identified to contain drizzle will also be more uncertain.

As seen in Fig. 4, the radiative heating rates can exceed the latent heating rates by an order of magnitude. The infrared cooling and latent heating terms are generally opposite in sign, so that near cloud-top, neglect of latent heating from droplet gravitational settling would generally lead to an overestimate of the total diabatic heating. In contrast, heating from shortwave absorption and condensation occur at similar vertical levels, and in these locations total diabatic heating is augmented by the consideration of gravitational settling. Below cloud base, radiative heating from higher-level infrared cloud emission is small, and evaporative cooling can be the dominant diabatic heating term.

4. Discussion

The latent heating term from droplet gravitational settling was found to be small relative to the radiative heating term, consistent with expectations for mostly non-drizzling conditions. Nevertheless, it is not negligible. The (non-drizzle) latent heating typically accounts for about 10% of the total diabatic heating, and below cloud base, it can be the dominant term.

It is possible that, despite the low radar reflectivities below the cloud base, most of the contribution to the radar reflectivity is from a few large drops, indicative of a very light drizzle. A separate liquid water flux calculation was done below cloud base using a drizzle estimate from the radar reflectivity: $Z = 1.2R^{1.14}$ where R is rain rate (R. Wood, pers. comm.). This increased the below-cloud-base liquid water fluxes by about a factor of five. While the Z-R relationship was not developed using dBZ $<$ -20, it does suggest that below cloud base the liquid water flux estimate from Eqn. (10) may be an underestimate.

During EPIC, significant drizzle was often found to evaporate completely below cloud base (Bretherton et al., 2003), and the associated latent cooling will be more pronounced than for the case examined here. Previous work has retrieved a vertically-resolved drizzle water flux from cloud radar measurements under stationary conditions (Frisch et al., 1995). The application of the technique to the unstabilized ship-board cloud radar of EPIC2001 is a more ambitious undertaking, however, as it also requires an accurate estimation of the contribution to the Doppler velocities caused by the ship-board motion.

We have ignored the second contribution in the flux term in Eqn. 1. This term includes the production of turbulent kinetic energy from the cloud-top radiative cooling, and is important. We will be using *in situ* aircraft measurements from the Dynamics and Chemistry of Marine Stratocumulus II experiment to see if we can determine the relative size of this contribution. In addition, the variations in N and σ_x reported in Frisch et al. (2002) were made from many aircraft flights under a variety of conditions. It may turn out that if we looked at these values for a certain time and location, these variations might be considerably smaller, reducing the error in our flux and latent heating estimates.

Acknowledgments We are grateful towards funding agencies for the support of this work. Shelby Frisch was supported by the NOAA Office of Global Programs and Paquita Zuidema was supported by a National Research Council Research Associateship Award.

REFERENCES

Beard, K. V. and H. R. Pruppacher, 1969: A determination of the terminal velocity and drag of small water drops by means of a wind tunnel. *J. Atmos. Sci.*, **26**, 1066–1071.

Bretherton, C. S., T. Uttal, C. Fairall, S. E. Yuter, R. A. Weller, D. Baumgardner, K. Comstock, and R. Wood, 2003: The EPIC stratocumulus study. *Bull. Amer. Meteor. Soc.* submitted; available through http://www.atmos.washington.edu/ breth/.

Frisch, A. S., C. W. Fairall, and J. B. Snider, 1995: Measurement of stratus cloud and drizzle parameters in ASTEX with a K_α-band Doppler radar and a microwave radiometer. *J. Atmos. Sci.*, **52**, 2788–2799.

Frisch, A. S., M. Shupe, I. Djalalova, G. Feingold, and M. Poellot, 2002: The retrieval of stratus cloud droplet effective radius with cloud radars. *J. Atmos. Oc. Tech.*, **19**, 835–842.

Key, J., 2001: Streamer user's guide. *Cooperative Institute for Meteorological Satellite Studies* 96 pp.

Nicholls, S., 1984: The dynamics of stratocumuls: aircraft observations and comparisons with a mixed-layer model. *Quart. J. Roy. Meteor. Soc.*, **110**, 783–820.